Colloid and Interface Science Communications 26 (2018) 7–13

Contents lists available at ScienceDirect

Colloid and Interface Science Communications

journal homepage: www.elsevier.com/locate/colcom

Self-Assembly Stereo-Specific Synthesis of Silver Phosphate Microparticles on Bacterial Cellulose Membrane Surface For Antimicrobial Applications

Bernardo Bayón[a], Maximiliano L. Cacicedo[a], Vera A. Álvarez[b], Guillermo R. Castro[a,*]

[a] Laboratorio de Nanobiomateriales, CINDEFI, Facultad de Ciencias Exactas, Universidad Nacional de La Plata - CONICET (CCT La Plata), Calle 47 y 115, B1900AJL La Plata, Argentina

[b] Grupo de Materiales Compuestos (CoMP), INTEMA (National Research Institute of Material Science and Technology), Facultad de Ingeniería, Universidad Nacional de Mar del Plata, Solís 7575, B7608FDQ Mar del Plata, Argentina

ARTICLE INFO

Keywords:
Bacterial cellulose
Antimicrobial activity
Drug delivery
Ciprofloxacin
Silver phosphate microparticles
Hybrid material

ABSTRACT

In situ self-assembly stereo-specific synthesis of silver phosphate (AgP) microparticles (MPs) in one side bacterial cellulose (BC) membrane surface and loading of ciprofloxacin provides BC scaffolds with a broad-spectrum antimicrobial activity against *Escherichia coli* and *Staphylococcus aureus*. The BC membranes containing AgP-MPs can be loaded > 5 times with ciprofloxacin compared to naked BC. The reuse of ciprofloxacin-loaded AgP-BC scaffolds in fresh cultures of both tested microbes showed high inhibition haloes without any signal of microbial resistance or scaffold activity decay after 30 days of assays. Additionally, microbial biofilms of *E. coli* and *S. aureus* were mostly killed by AgP-BC scaffolds loaded with ciprofloxacin in 1 h. The biophysical characterization of the hybrid AgP-BC scaffolds was performed by scanning electron microscopy (SEM), vibrational spectroscopy (FTIR), calorimetric techniques and X-ray diffraction (XRD). SEM images display AgP-MP spheroid structures with a high homogenous distribution on BC scaffold surfaces. The properties of the novel AgP-BC matrices are very promissory for biomedical applications, like a therapeutic dressing patches for the prevention and treatment of microbial infections in skin wounds and burns.

1. Introduction

The world population suffering chronic ulcers, scalds, severe burns and wounds is rising because of an adverse social impact in many low- and middle-income countries that is challenging medical and research areas. Particularly, skin wound therapies are one of the riskiest treatments in episodic and chronic pathologies such as diabetes, severe burns and others, mostly in medium/long-term hospitalized patients because of the high probability to suffer bacterial infections. For example, approximately 265,000 diseases per year were caused only by skin burns in low- and middle-income countries according to the World Health Organization (WHO) 2017 report. Furthermore, in 2014 the WHO reported 422 million people worldwide with diabetes consuming between 15% and 25% of the health care resources in their countries. Also, at least 25% of diabetic patients develop chronic ulcers during their lifetime, and the ultimate consequence without proper care is that they must undergo lower limb amputations. Since open wounds are the preferred access of pathogens to be spread in the body, the first and main therapeutic approach is the systemic and local administration of drugs. Besides, systemic drug administration sometimes does not provide an optimal therapy because of the high concentration of pathogens localized in the wounds and the presence of multidrug resistant (MDR) microorganisms. Additionally, due to the prevalence of MDR microorganisms in many pathologies around the world, the WHO declared a global antibiotic emergency.

Local treatment using transdermal patches combining therapeutic molecules and containing different biocide principles can be excellent alternatives to treat MDR microorganisms with high efficiency, low costs of production, ease of manipulation and replacement without the requirement need for specific medical facilities and trained personnel. Transdermal patches for different applications with contraceptive and anticholinergic activities and containing nicotine to treat tobacco addiction are available on the market.

Bacterial cellulose (BC) is a natural polymer biosynthesized by many microorganisms, but the most popular is *Komagataeibacter hansenii* (formerly *Gluconacetobacter hansenii*) [1, 2]. BC is composed of pure cellulose nanofiber mesh consisting of β-(1 → 4) glucose chains that is synthesized at the air/liquid interface as a three-dimensional asymmetric network of nanofibrils during bacterial growth [2, 3]. The BC matrix structure has a high-water content (about 99%) and displays

* Corresponding author.
E-mail address: grcastro@quimica.unlp.edu.ar (G.R. Castro).

https://doi.org/10.1016/j.colcom.2018.07.002
Received 19 April 2018; Received in revised form 4 July 2018; Accepted 11 July 2018

distinctive properties such as high purity, high degree of polymerization (up to 8000 glucose units), high crystallinity (70%–80%) and mechanical stability. The BC high water content and purity make the matrix biocompatible for multiple medical applications, particularly for tissue engineering and skin wound healing [4, 5]. However, native BC has no antimicrobial activity. In the last decade, BC composites showing biological activity were explored particularly for skin repair and tissue engineering. The most common polymers to tailor BC scaffolds are alginates, hyaluronic acids and gelatins. The addition of polymers to BC confers novel and interesting properties to the scaffolds including mucoadhesivity and the ability of being a molecular carrier [5, 6].

The interest in silver as an antibacterial agent, used since ancient times, was recently rediscovered by research community and extensively studied in the last ten years [7, 8]. The main advantages of silver devices are based on their low toxicity to humans, broad antimicrobial spectrum and low probability to produce bacterial resistance compared to traditional antimicrobials. In fact, silver alone or combined with other molecules is currently used for controlling bacterial growth in a variety of applications, including dental implants, catheters, skin creams and clothes [9]. The strong silver biocide activity was attributed to several antimicrobial mechanisms such as damage of cell scaffold proteins, blocking of RNA transcription, disruption of DNA binding and replication [10].

Metallic silver nanoparticles with a diameter between 20 nm and about 110 nm showed different cytotoxic values, but in all cases cellular and/or inflammatory response and/or genotoxicity in mammalian cells were reported [11, 12] The toxicity of metallic silver nanoparticles was associated with the cellular uptake of Ag^{+1} acting inside the cells [13]. Also, the toxicity of the metallic silver nanoparticles was inversely proportional to de diameter of the nanoparticles. Metallic silver nanoparticles of low dimensions (i.e., 10 nm diameter) were much more toxic than particles of large diameters [11, 13].

Silver phosphate microparticles (AgP-MPs) developed in our laboratory are in the size range of 1.3 μm to 1.5 μm (with a distribution higher than 90% of the microparticle population) and at least 14 times bigger than metallic silver nanoparticles but with similar bactericidal effect [14]. Another advantage of AgP-MPs is that they are a mesoporous material with the ability to absorb and contain molecules with different molecular weights and physicochemical properties keeping their biological activities. The tuning of mesoporous structures determines the interactions within the loads and consequently, the controlled release kinetics [15].

Hybrid devices based on silver salts and polymers could improve the antimicrobial activity against pathogens, but only few reports can be found in the literature and the mechanisms are not fully understood [16, 17]. Among biopolymers, alginate, cellulose, pectin and others were lately reported as potential “green carriers” for drug delivery [18]. Natural polymers provide excellent platforms for molecular loading and release because of their gelling properties, GRAS status by FDA, and some of them can be considered smart molecules since they are responsive to environmental conditions (e.g., pH, temperature, ionic strength).

Fluoroquinolones comprise a large family of antibiotics widely used for the treatment of microbial infections in mammals because they inhibit DNA gyrase and topoisomerase IV present only in bacteria and cause microbial cell death. The second-generation fluoroquinolones such as ciprofloxacin (Cipro) were considered the worldwide battle horse for the treatment of bacterial infections. Besides, the oral administration of Cipro requires high antibiotic doses because of low antibiotic solubility and the trend to π-stacking causing low drug bioavailability and gastrointestinal associated problems. The encapsulation of fluoroquinolones seems to be an alternative to reduce the undesirable secondary effects and extend the drug release. Particularly, gel structures have been reported to be efficient for the encapsulation of fluoroquinolones increasing antibiotic efficiency, reducing the antibiotic dose, and extending the antimicrobial activity of the antibiotic [19, 20]. In previous work in our laboratory, mesoporous AgP-MPs were developed for the encapsulation of levofloxacin showing high drug encapsulation efficiency, high surface area, small pore size, and high bactericidal activity [14].

The aim of the present work was to develop bacterial cellulose scaffolds containing a dual antimicrobial activity conferred by self-assembly of silver phosphate microparticles and ciprofloxacin for potential application in skin wound/burn dressing. The BC systems were characterized by infrared spectroscopy (FTIR), thermogravimetric analysis (TGA), X-ray diffraction (XRD) and scanning electron microscopy (SEM). Ciprofloxacin loading on BC scaffolds and kinetic release from the matrices were analyzed. Antimicrobial assays were carried out with *Escherichia coli* (Gram(−) bacteria) and *Staphylococcus aureus* (Gram(+) bacteria), the main causative agents of skin infections.

2. Materials and Methods

2.1. Chemicals and Media

All reagents used were of analytical grade purchased from Sigma (St. Louis, MO, USA), Merck (Darmstadt, Germany) or local suppliers. Deionized water was prepared using reverse osmosis equipment Aqual 25 (Brno, Czech Republic) and further purified by using MilliQ Direct QUV apparatus equipped with a UV lamp.

2.2. Bacterial Cellulose

The synthesis of bacterial cellulose (BC) by *Komagataeibacter hansenii* (ATCC 23769) was performed in a medium containing ($g\,l^{-1}$): 25.0 mannitol, 5.0 yeast extract, 3.0 peptone, and adjusted to pH = 6.5 with 0.1 M NaOH solution before sterilization. The culture was maintained statically in 96-well plates at 30 °C for 6 days. The BC membranes were collected from the plates and washed with distilled water. BC purification was performed by incubating the scaffolds in 100 mM NaOH at 50 °C for 24 h followed by successive washes with distilled water and adjustment of the pH to 7.0. Later, the BC membranes were sterilized by autoclaving (121 °C for 20 min).

2.3. Synthesis of Silver Phosphate Microparticles in BC Scaffolds

The BC system containing nanostructured micro-hybrid particles (AgP-Ms) was developed by colloidal crystallization in the presence of sodium tripolyphosphate (Na-TPP) as follows: BC membranes were immersed in a vial containing 60 mM sodium tripolyphosphate ($Na_5P_3O_{10}$) at 25 °C for 20 min under low speed stirring. Later, a solution containing 100 mM $AgNO_3$ was poured into the vial, and stirred at 250 rpm for other 20 min. Each BC film was washed twice with distilled water.

2.4. Infrared Spectroscopy (FTIR)

BC membranes were examined in an infrared spectrometer (Thermo Scientific Nicolet 6700) equipped with attenuated total reflection (ATR). The samples were analyzed at room temperature in the 400–4000 cm^{-1} spectral range with 4 cm^{-1} resolution and 32 scans.

2.5. X-Ray Diffraction (XRD) Analysis

The crystal diffraction patterns of dried scaffold samples were collected using Analytical Expert Instrument (Philips 3020, The Netherlands) using CuKα radiation (1.54 Å) and scans in the 2Θ range 0° to 60° with 0.04 step size and 1.00 seg/s/step at room temperature. The generator voltage and the current were set at 40 kV and 35 mA respectively at room temperature.

2.6. Thermal Analysis (TGA)

Dynamic thermogravimetric measurements of native and hybrid bacterial cellulose scaffolds were performed by using a Universal TGA 500 (TA Instruments, New Castle, DE, USA). Tests were carried out from 20 °C to 600 °C at a constant heating rate of 10 °C/min under N_2 atmosphere [21].

2.7. Scanning Electron Microscopy (SEM)

The morphology and structural scaffold analysis was performed by SEM using freeze-dried scaffolds. Prior to the freeze-drying procedure, the membranes were frozen in liquid nitrogen, then freeze-dried for 72 h and finally stored in desiccators under dark conditions till SEM analysis. The samples were prepared by sputtering scaffold with gold using a Balzers SCD 030 metalizer with a layer thickness between 15 and 20 nm. The scaffold surface and morphologies were observed using Philips SEM 505 model (Rochester, USA), and processed by an image digitizer program (Soft Imaging System ADDA II (SIS)).

2.8. Energy Dispersive X-Ray Analysis (EDAX)

The chemical analysis by EDAX was performed on dried samples using Apex 2 EDAX Apollo X coupled to SEM.

2.9. Drug Loading Studies

Bacterial scaffolds (diam. = 6.9 mm) were immersed in 1.0 mg/ml Cipro solutions and stirred at 80 rpm at 5 °C for 24 h. Later, the BC scaffolds were taken out from the vials, and residual Cipro was assayed in the supernatants using a spectrofluorometer (Tecan, Germany) employing λ_{exc} = 280 nm and λ_{em} = 460 nm with appropriate calibration curves. Scaffolds were washed 3 times in water. The loading efficiency was evaluated as follows:

$$\text{Cipro Incorporation} = \frac{(\text{Cipro}^0 - \text{Ciprox}) \times 100}{\text{Cipro}^0} \quad (1)$$

where Cipro^0 and Cipro^x are antibiotic concentrations (μmol) in the solution at the initial time (t_0) and at time ($t_x > 0$) after removing the loaded scaffold respectively.

2.10. In Vitro Drug Release Studies

BC scaffolds were placed in 10 ml of simulated normal skin pH (e.g., 50 mM acetate buffer, pH = 5.5) in 15-ml Falcon tubes and incubated at 37 °C. Samples of 30 μl were withdrawn and refilled with an equal volume of fresh buffer at defined intervals. Cipro kinetic release from the matrices was determined as mentioned before and performed in triplicate for each system.

2.11. Antimicrobial Assays of Ag_3PO_4 MPs Loaded with Ciprofloxacin

Cipro was loaded into the BC scaffolds containing or not silver phosphate microspheres to test antimicrobial activity against *S. aureus* and *E. coli*, typical Gram(+) and Gram(−) bacteria. The scaffolds were further placed on the inoculated nutrient agar plate surface and also containing standard ciprofloxacin disks. The plates were incubated at 37 °C and then the inhibition zones were determined after 24 h. The inhibition zones were measured and compared using ImageJ software. The residual antimicrobial activity of AgP-BC scaffolds was tested using an identical procedure one month later.

The effect of AgP-MPs on microbial biofilms was analyzed using commercial kit Live/dead BacLight® composed of two fluorescent dyes: SYTO9® (green color) to stain live cells and propidium iodide (red color) to stain DNA (i.e., dead cells).

For the microbiological assays, *S. aureus* and *E. coli* growing at late exponential phase were inoculated in a soft nutrient agar, and a 20-μl drop of culture medium was placed on the surface of a glass slide, followed by incubation for 24 h to allow biofilm formation. Subsequently, the microbial biofilms were covered with the AgP-BC scaffolds with or without Cipro for 30, 60 min and 24 h. After treatment, biofilms were carefully removed and washed with deionized water.

Biofilm staining was developed with a mixture of both dyes prepared in equal proportions (0.75 μl of each one in 500 μl of sterile deionized water) and applied onto the entire biofilm and held in darkness for 20 min. Then, the samples were washed with deionized water and observed in an epifluorescence microscope (Leica DM 2500, Germany) equipped with UV filter (495–505 nm) to determine the cell viability of bacteria. The filters used were U-MWG2 ($\Delta\lambda_{excitation\ max}$ = 510–550 nm and $\lambda_{emission\ max}$ = 590 nm), for observing live bacteria (green), and U-MWB2 ($\lambda_{excitation\ max}$ = 460 and $\Delta\lambda_{emission\ max}$ = 490–520 nm) to observe damaged bacteria (red).

2.12. Statistical Analysis

All experiments were carried out at least twice in duplicate or triplicate. Comparisons of the means were performed by analysis of variance (ANOVA) with a significance level of 5.0% ($p < .05$) followed by Fisher's least significant difference test at $p < .05$.

3. Results and Discussion

3.1. Surface Morphology of BC Scaffolds

SEM and EDAX images of BC and AgP-BC scaffold composites display very different topological characteristics for both matrix structures, confirming the presence of silver phosphate in the BC scaffold (Fig. 1 and Fig. 1S). SEM microphotographs of naked BC show cross-linked fibrous BC membrane structures with many free fibers (Fig. 1A). Meanwhile, silver phosphate microparticles are fully covering only one side of the cellulose membrane (Fig. 1B and C). The asymmetric synthesis of AgP-NPs in the cellulose matrix can be explained in terms of the synthesis of cellulose by the microorganism in liquid media. The bacteria growing in liquid media produce cellulose microfibrils that go to the air-liquid interphase where the microfibrils in the liquid media are entangled, forming the cellulose membrane structure. After the purification procedures in which bacteria were eradicated from the cellulose membrane, the growing chains of β-glucose are pending from the matrix (i.e., like a comb) and remain free to be easily derivatized. The BC pending nanofibers act as nucleation centers for the growth of AgP-MPs. This self-assembly procedure allows the coverage of the cellulose fibers with a homogeneous spherical distribution of microparticles on one side of the BC membrane only (Fig. 1B).

The analysis of AgP-BC scaffolds by EDAX confirmed the presence of silver and phosphorous as major components of the BC matrix (Fig. 1S, Supplementary Material). There is also a sodium peak from sodium triphosphate as previously reported [14].

3.2. Thermal Analysis (TGA)

TGA and DTGA curves for BC and AgP-BC MP scaffolds are displayed in Fig. 2. It can be observed that both kind of materials display only one degradation step, with the most important weight loss in the range of 315 °C to 350 °C and centered at around 308 °C. This pronounced weight loss is attributed to the thermal degradation of BC. In addition, the obtained curves show that the weight loss is reduced in the case of the membranes containing the microparticles. Whereas the weight loss for BC was around 82% for BC in the organic range (between 200 and 500 °C), the same parameter was near to 12% for AgP-BC MP scaffolds. Another conclusion is that the incorporation of AgP

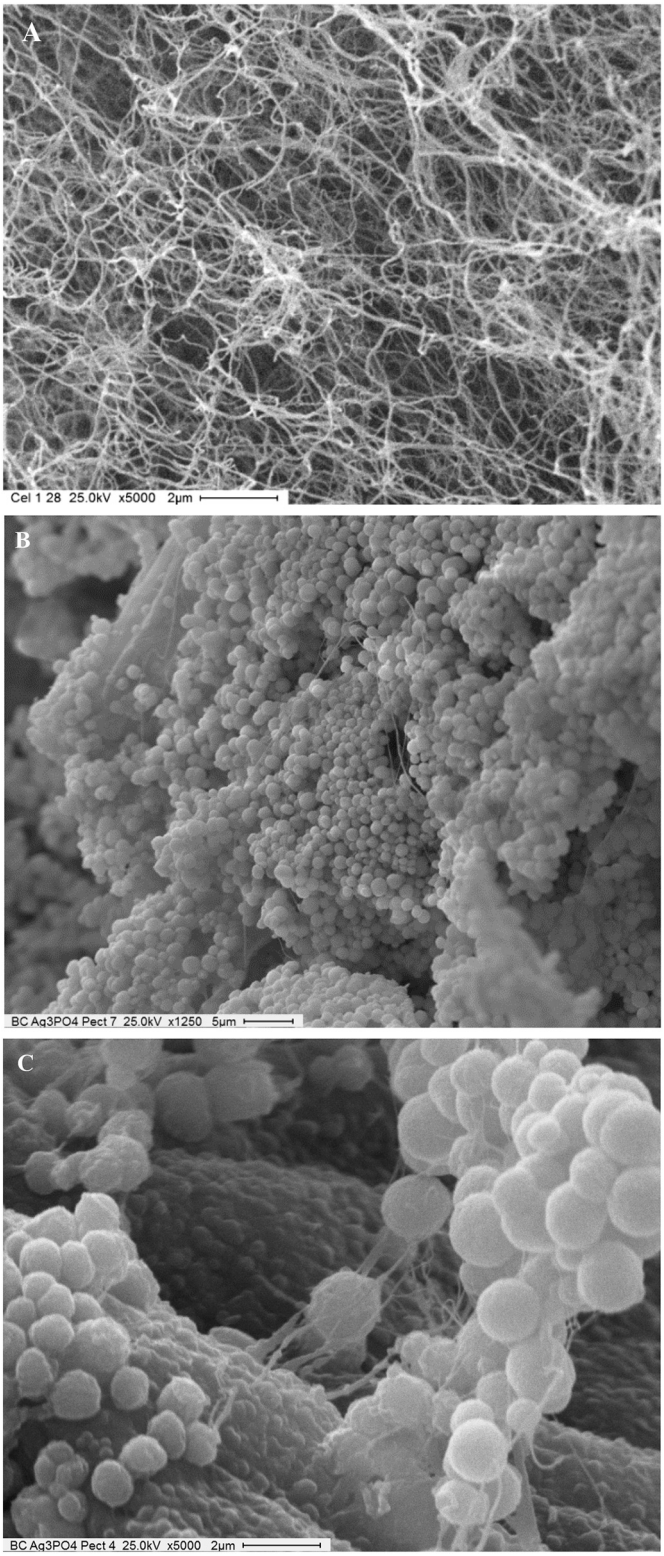

Fig. 1. Scanning electron microscopy microphotographies of bacterial cellulose membranes: naked (A) and decorated with silver phosphate microparticles (B and C).

produces a reduction in the hydrophilicy of the material that can be associated with the first weight loss (between room temperature and 170 °C) which is related to the vaporization of water molecules from the material. The as observed behavior could be related to covering of inorganic nanoparticles on the BC scaffold surface making a shield that.

3.3. X-Ray Diffraction Analysis

The XRD analysis was carried out to elucidate potential structural changes in the BC scaffolds by the presence of AgP-MPs (Fig. 3). The diffractograms were compared to the standard, and the major diffraction peaks of the composite material samples were in line with the standard spectrum of the Ag_3PO_4 (JCPDS card No. 06-0505) and shown in Fig. 3. The distinctive peaks at 29.696°, 33.293°, 36.588°, 47.792°, matched with the standard ones shows on jcpds of Ag_3PO_4. These results evidenced the presence of silver phosphate in the BC scaffolds containing the microparticles, similarly as previously reported for free silver phosphate microparticles [1]. In addition, BC not only does not affect the nucleation of silver microparticles in solution but also in fact BC is acting as a support for the silver phosphate microparticle in-situ synthesis.

3.4. Infrared Spectroscopy (FTIR) of Bacterial Cellulose Scaffolds

The interaction between bacterial cellulose and silver phosphate microparticles was studied by FTIR. The main peak assignments are listed in Table 1 and Table 1S. The comparison of Ag_3PO_4 and AgP-BC FTIR spectra showed a high displacement of most of the wavenumbers indicating a strong interaction between the salt within the residues of the biopolymer. Two main characteristics can be observed depending on the groups involved: the wavenumbers of Ag_3PO_4 attached to the cellulose scaffold increase indicating a hypsochromic shift for the nonpolar P-O-P symmetric and asymmetric stretching modes. On the other hand, vibrational bands of polar and polarizable residues, such as $(PO_3)^{-4}$, $(PO_3)^{-2}$ and P═O, in contact with cellulose scaffolds display bathochromic shift (to lower wavenumbers) (Table 1). Both types of displacement can be explained in terms of the high hydrophilicity of the bacterial cellulose matrices because of the high number of hydroxyl groups interacting synergically with polar and/or polarizable residues of the phosphate molecule. However, nonpolarizable residues (e.g., P—O—P) of phosphate are not able to interact within the polar groups of cellulose. Also, the comparison of FTIR spectra of naked BC with AgP-BC scaffolds showed a strong presence of silver phosphate particles covering all scaffold surfaces but hiding the native cellulose peaks because of the low sensitivity of the FTIR-ATR technique. Table 1S lists the characteristic vibrational modes of BC [21].

3.5. Ciprofloxacin Loading on Bacterial Cellulose and Release Assays

The loading of naked BC scaffolds with Cipro was only 5.0%. The incorporation of AgP-MPs into the BC membrane increased Cipro loading higher than six-folds (Table 2).

The ciprofloxacin kinetic release of naked BC and AgP-BC was evaluated at pH 5.5, which corresponds to the normal pH of human skin. The Cipro release from BC membranes showed a burst size release during the first 4 h of incubation, while the release profile of Cipro from the AgP-BC increased slowly at least until 70 h (Fig. 4).

3.6. Antimicrobial Assays

The antimicrobial activity of AgP-BC was tested in agar plates spread with *S. aureus* and *E. coli*. Bacterial cellulose membranes were placed as negative control, also a standard disk containing ciprofloxacin was used as a positive control. The antimicrobial activity comparison of AgP-BC scaffolds loaded or unloaded with Cipro in agar plates shows high and similar inhibition haloes for both *E. coli* and *S. aureus* plates respectively indicating that diffusion phenomenon do not predominate (Fig. 5 and Fig. 2S). Besides, the antimicrobial activity of Cipro is highly enhanced by the presence of AgP-MPs attached to the BC scaffolds.

Furthermore, the residual activity of AgP-BC was tested employing the same scaffolds previously used in a new inoculated medium having similar bactericidal effects for at least one month (Fig. 3S).

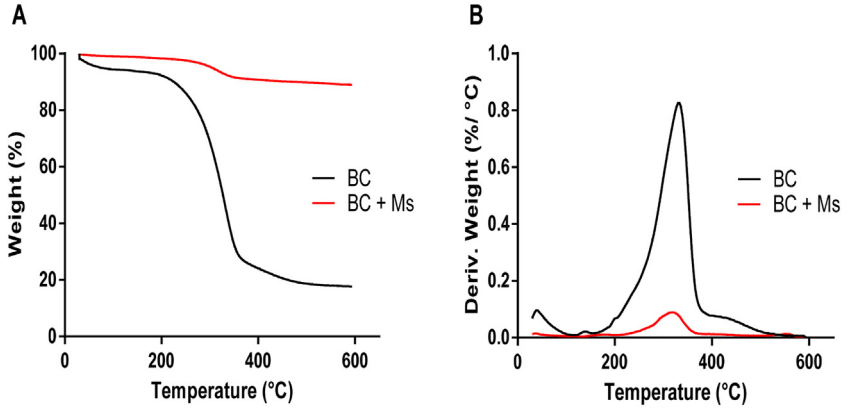

Fig. 2. Thermogravimetric assay of bacterial cellulose, bacterial cellulose containing silver phosphate. **A**) Weight (%) vs T(°C); **B**) Weight derivate (%/°C) vs T(°C).

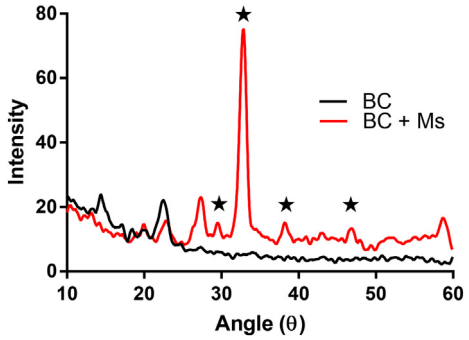

Fig. 3. X-Ray diffraction profiles of naked bacterial cellulose (black) and bacterial cellulose with silver phosphate microparticles (red). (For interpretation of the references to color in this figure legend, the reader is referred to the web version of this article.)

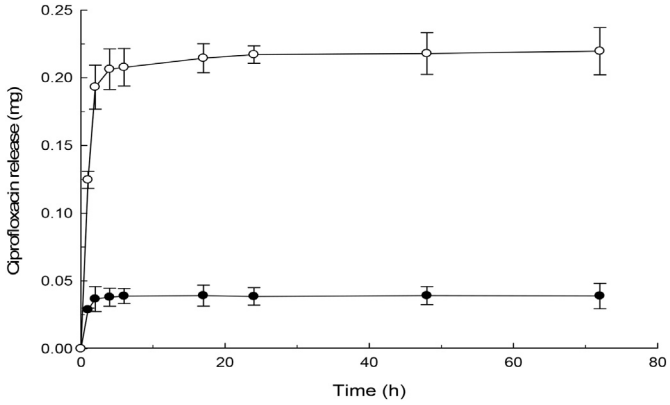

Fig. 4. Kinetic of ciprofloxacin release from bacterial cellulose membranes containing (○) or not (●) silver phosphate microparticles.

Table 1
FTIR assignments of bacterial cellulose membranes: Ag_3PO_4 microparticles, BC containing Ag_3PO_4 microparticles respectively and the difference between them (Δ).

Assignments	Wavenumbers (cm^{-1})		
	Ag_3PO_4 (1)	AgP-BC (2)	$\Delta\bar{\upsilon} = \bar{\upsilon}(1) - \bar{\upsilon}$ (2)
Symmetric stretching vibration of P–O–P linkage	629	707	−78
Asymmetric stretching vibration of P–O–P linkage	886	896	−10
Vibration modes of $(PO_3)^{-4}$ group	1042	975	+66
Asymmetric stretching modes of chain terminating $(PO_3)^{-2}$	1088	1005	+82
Asymmetric stretching of double bonded PO modes	1261	1074	+186

Table 2
Ciprofloxacin loading efficiency on bacterial cellulose (BC) membranes containing or not silver phosphate microparticles.

Membrane type	Loading efficiency (%)
BC	5.0 ± 0.4
AgP-BC	30.0 ± 0.2

Interestingly, no resistant bacteria colonies of both tested microorganisms were observed inside the inhibition haloes produced by a combination of loaded Cipro into AgP-BC scaffolds. This result can be interpreted by the synergistic effect of the antimicrobial activity of AgP plus the effect of the antibiotic.

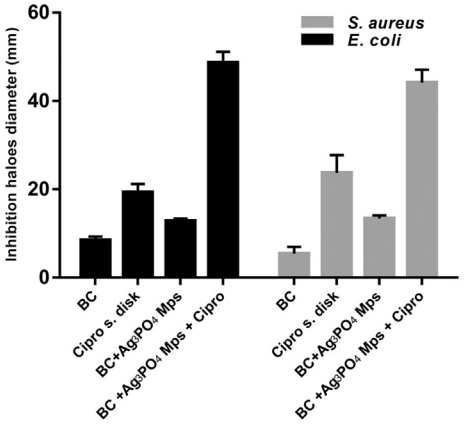

Fig. 5. Inhibition haloes (diameter) of bacterial cellulose membranes (BC), ciprofloxacin commercial standard disks (Cipro s. disks), bacterial cellulose having silver phosphate microparticles (BC+ Ag_3PO_4 Mps) and bacterial cellulose containing silver phosphate microparticles and ciprofloxacin (BC + Ag_3PO_4 Mps + Cipro) on agar plate inoculated with *S. aureus* and *E. coli* after incubation at 37 °C for 24 h.

Moreover, the antimicrobial activity of AgP-BC on bacterial biofilms was tested with the Live/Dead kit (Fig. 6). The untreated biofilms of *Escherichia coli* and *Staphylococcus aureus* display bright green fluorescent stain indicating live bacteria. However, after the biofilm exposure to AgP-BC for 30 min, a red population begins to appear, indicating the presence of damaged bacteria with loss of cell membrane integrity (data not shown). One hour later, only few green spots were observed on the plates and mainly surrounded by a strong red color,

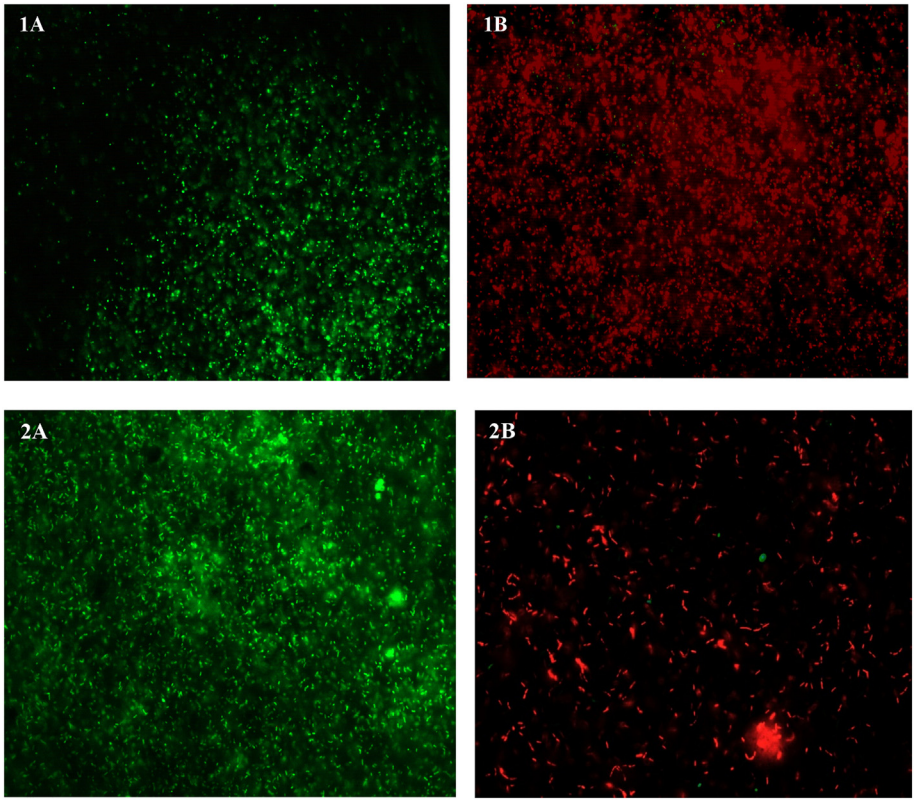

Fig. 6. Survival experiments of *S. aureus* (1) and *E. coli* (2) biofilms before (A) and after 1-hour treatment (B) with bacterial cellulose membranes containing silver phosphate microparticles.

indicating that most of the bacteria in the biofilm are dead after treatment with AgP-BC (Fig. 6).

4. Conclusions

A new hybrid material based on bacterial cellulose containing silver phosphate microparticles on one side of the matrix and high ciprofloxacin loading has been developed. The AgP-MPs developed by the self-assembly technique on only one side of the bacterial cellulose surface provide a novel and promising composite material with excellent antimicrobial activity against both Gram(+) and Gram(−) bacteria. BC membranes showed relevant properties such as non-adhesive hydrogel dressing capability, high skin tissue compatibility, excellent water uptake ability, high mechanical strength and air permeability. Additionally, hybrid AgP-BC scaffolds were made by a green chemistry synthesis procedure under controlled physicochemical conditions, using a reproducible and facile preparation method. The antimicrobial activity of BC is directly related to the presence of silver microspheres.

The mesoporous silver phosphate hybrid microspheres synthesized on the surface of bacterial cellulose fibers have spherical shape, confirmed by microscopy techniques (SEM). The X-ray diffraction patterns of BC scaffolds containing silver phosphate microparticles showed no changes in the crystal structure of Ag_3PO_4 by the presence of cellulose. The thermal analysis yielded the results expected from the incorporation of inorganic microspheres in the surface of cellulose fibers. Another advantage of the BC-Ag_3PO_4 membranes is their ability to load molecules, which can be associated with desirable biological activities as antibiotics, ciprofloxacin in our case. The enhanced incorporation of ciprofloxacin into the scaffolds can be attributed only to the presence of silver phosphate microspheres.

As the silver phosphate microparticles are a mesoporous materials and have a large surface/volume ratio, this property gives the microparticles the ability to absorb different molecules in its pores. In this case, the advantage of this feature is the ability of encapsulate an antibiotic such as ciprofloxacin. Also, the particles have the well-known antimicrobial property of the silver particles, therefore the idea is to enhance the antimicrobial activity of the antibiotic combined with silver. The drug is entrapped in the surface pores of the microparticles and released by to the surrounding zones by passive mechanism.

The antimicrobial effect of the AgP-BC scaffolds loaded with ciprofloxacin was their high biocide activity against *E. coli* and *S. aureus* without any sign of microbial resistance for at least one month. The results on microbial biofilms exposed to the membranes with microparticles and loaded with Cipro demonstrated a strong antimicrobial effect on bacteria. The biocide mechanism could be explained considering the structural instability of the bacterial membrane caused by the contact and/or diffusion of silver ions that improves the diffusion of ciprofloxacin inside the bacteria cells causing strong inhibition of DNA gyrase and topoisomerase IV and consequently, enhancing bacterial cell death.

The main advantage of AgP-BC scaffolds loaded with Cipro is the synergic antimicrobial effect of the silver ion with fluoroquinolone in the same microdevice with dual function as a biocide matrix and as carrier for an antibiotic (i.e., ciprofloxacin). The hybrid system developed could have potential applications in the biomedical field for skin wound/burn dressing, particularly for pathologies with chronic skin injuries and ulcers (i.e., diabetes).

Acknowledgments

The present work was supported by Argentine grants from CONICET (National Council for Science and Technology, PIP 0498), The National Agency of Scientific and Technological Promotion (ANPCyT, Grant # PICT2011-2116), Fundación Argentina de Nanotecnología (FAN, Europaid/135085/M/ACT/AR), and UNLP (National University of La Plata, 11/X545) to GRC.

Appendix A. Supplementary data

Supplementary data to this article can be found online at https://doi.org/10.1016/j.colcom.2018.07.002.

References

[1] N. Petersen, P. Gatenholm, Bacterial cellulose-based materials and medical devices: current state and perspectives, Appl. Microbiol. Biotechnol. 91 (2011) 1277–1286, https://doi.org/10.1007/s00253-011-3432-y.

[2] M.L. Cacicedo, I.E. León, J.S. Gonzalez, L.M. Porto, V.A. Alvarez, G.R. Castro, Modified bacterial cellulose scaffolds for localized doxorubicin release in human colorectal HT-29 cells, Colloids Surfaces B Biointerfaces 140 (2016) 421–429, https://doi.org/10.1016/j.colsurfb.2016.01.007.

[3] H.S. Barud, T. Regiani, R.F.C. Marques, W.R. Lustri, Y. Messaddeq, S.J.L. Ribeiro, Antimicrobial bacterial cellulose-silver nanoparticles composite membranes, J. Nanomater. 721 (2011) 631–639, https://doi.org/10.1155/2011/721631.

[4] L. Fu, J. Zhang, G. Yang, Present status and applications of bacterial cellulose-based materials for skin tissue repair, Carbohydr. Polym. 92 (2013) 1432–1442, https://doi.org/10.1016/j.carbpol.2012.10.071.

[5] M. Mustafa, M. Cairul, I. Mohd, C. Martin, A review of bacterial cellulose-based drug delivery systems: their biochemistry, current approaches and future prospects, J. Pharm. Pharmacol. 66 (2014) 1047–1061, https://doi.org/10.1111/jphp.12234.

[6] N. Chiaoprakobkij, N. Sanchavanakit, K. Subbalekha, P. Pavasant, M. Phisalaphong, Characterization and biocompatibility of bacterial cellulose/alginate composite sponges with human keratinocytes and gingival fibroblasts, Carbohydr. Polym. 85 (2011) 548–553, https://doi.org/10.1016/j.carbpol.2011.03.011.

[7] O. Choi, K.K. Deng, N.-J. Kim, L. Ross, R.Y. Surampalli, Z. Hu, The inhibitory effects of silver nanoparticles, silver ions, and silver chloride colloids on microbial growth, Water Res. 42 (2008) 3066–3074, https://doi.org/10.1016/j.watres.2008.02.021.

[8] W.-R. Li, X.-B. Xie, Q.-S. Shi, H.-Y. Zeng, Y.-S. Ou-Yang, Y.-B. Chen, Antibacterial activity and mechanism of silver nanoparticles on *Escherichia coli*, Appl. Microbiol. Biotechnol. 85 (2010) 1115–1122, https://doi.org/10.1007/s00253-009-2159-5.

[9] M.H. El-Rafie, H.B. Ahmed, M.K. Zahran, Characterization of nanosilver coated cotton fabrics and evaluation of its antibacterial efficacy, Carbohydr. Polym. 107 (2014) 174–181, https://doi.org/10.1016/j.carbpol.2014.02.024.

[10] P.D. Marcato, R. De Conti, O.L. Alves, F.T.M. Costa, M. Brocchi, Potential use of silver nanoparticles on pathogenic bacteria, their toxicity and possible mechanisms of action, J. Braz. Chem. Soc. 21 (2010) 949–959.

[11] A.R. Gliga, S. Skoglund, I.O. Wallinder, B. Fadeel, H.L. Karlsson, Size-dependent cytotoxicity of silver nanoparticles in human lung cells: the role of cellular uptake, agglomeration and Ag release, Part. Fibre Toxicol. 11 (1) (2014), https://doi.org/10.1186/1743-8977-11-11.

[12] M.V.D.Z. Park, A.M. Neigh, J.P. Vermeulen, L.J.J. De, H.W. Verharen, J.J. Briedé, et al., The effect of particle size on the cytotoxicity, inflammation, developmental toxicity and genotoxicity of silver nanoparticles, Biomaterials 32 (2011) 9810–9817, https://doi.org/10.1016/j.biomaterials.2011.08.085.

[13] A. Ivask, I. Kurvet, K. Kasemets, I. Blinova, V. Aruoja, S. Suppi, et al., Size-dependent toxicity of silver nanoparticles to bacteria, yeast, algae, crustaceans and mammalian cells in vitro, PLoS One 9 (2014) 102–108, https://doi.org/10.1371/journal.pone.0102108.

[14] B. Bayón, V. Bucalá, G.R. Castro, Development of antimicrobial hybrid mesoporous silver phosphate–pectin microspheres for control release of levofloxacin, Microporous Mesoporous Mater. 226 (2016) 71–78, https://doi.org/10.1016/j.micromeso.2015.12.041.

[15] S.Y. Park, M. Barton, P. Pendleton, Mesoporous silica as a natural antimicrobial carrier, Colloids Surfaces A Physicochem. Eng. Asp. 385 (2011) 256–261, https://doi.org/10.1016/j.colsurfa.2011.06.021.

[16] R. Ladj, A. Bitar, M.M. Eissa, H. Fessi, Y. Mugnier, R. Le Dantec, et al., Polymer encapsulation of inorganic nanoparticles for biomedical applications, Int. J. Pharm. 458 (2013) 230–241, https://doi.org/10.1016/j.ijpharm.2013.09.001.

[17] Y. Murali Mohan, K. Vimala, V. Thomas, K. Varaprasad, B. Sreedhar, S.K. Bajpai, et al., Controlling of silver nanoparticles structure by hydrogel networks, J. Colloid Interface Sci. 342 (2010) 73–82, https://doi.org/10.1016/j.jcis.2009.10.008.

[18] C. Alvarez-Lorenzo, B. Blanco-Fernandez, A.M. Puga, A. Concheiro, Crosslinked ionic polysaccharides for stimuli-sensitive drug delivery, Adv. Drug Deliv. Rev. 65 (2013) 1148–1171, https://doi.org/10.1016/j.addr.2013.04.016.

[19] G.A. Islan, I.P. De Verti, S.G. Marchetti, G.R. Castro, Studies of ciprofloxacin encapsulation on alginate/pectin matrixes and its relationship with biodisponibility, Appl. Biochem. Biotechnol. 167 (2012) 1408–1420, https://doi.org/10.1007/s12010-012-9610-2.

[20] Y.N. Martinez, L. Pinuel, G.R. Castro, J.D. Breccia, Polyvinyl alcohol-pectin cryogel films for controlled release of enrofloxacin, Appl. Biochem. Biotechnol. 167 (2012) 1421–1429, https://doi.org/10.1007/s12010-012-9554-6.

[21] S. Saska, H.S. Barud, A.M.M. Gaspar, R. Marchetto, S.J.L. Ribeiro, Y. Messaddeq, Bacterial cellulose-hydroxyapatite nanocomposites for bone regeneration, Int. J. Biomater. 9 (2011), https://doi.org/10.1155/2011/175362.